Effect of ZnSe/GaAs interface treatment in ZnSe quality control for optoelectronic device applications

Kwangwook Park[1], Daniel Beaton[1], Kenneth X. Steirer[1], and Kirstin Alberi[1, *]

[1]National Renewable Energy Laboratory, Golden, Colorado 80401, United States

[*]E-mail: kirstin.alberi@nrel.gov

Abstract

We investigate the role of interface initiation conditions on the growth of ZnSe/GaAs heterovalent heterostructures. ZnSe epilayers were grown on GaAs surface with various degrees of As-termination and the application of either a Zn or Se pre-treatment. Structural analysis revealed that Zn pre-treatment of an As-rich GaAs surface suppresses Ga_2Se_3 formation at the interface and promotes the growth of high crystal quality ZnSe. This is confirmed with low-temperature photoluminescence. However, moderation of Ga-Se bonding through a Se pre-treatment of an As-rich GaAs surface can prevent excessive intermixing at the interface and promote excitonic emission in the underlying GaAs layer. These results provide guidance on how best to prepare heterovalent interfaces for various applications.

Introduction

Semiconductor interfaces play a critical role in the performance of optoelectronic devices. When designed and fabricated correctly, they offer the ability to engineer band offsets and free carrier profiles that can enhance device functionality. Incorrect implementation, however, can lead to excess defect generation and carrier recombination that could render the device useless. Heterovalent III-V/II-VI interfaces exemplify both of these advantageous and disadvantageous aspects. Many combinations of III-V and II-VI compounds and alloys can be lattice matched to one another, allowing them to be integrated into epitaxial structures. II-VI semiconductors also typically have higher bandgap energies than their lattice-matched III-V counterparts, providing an avenue to create type I heterojunctions with large offset potentials that could be used for cladding and window layers. Yet, perfect II-V and III-VI bonding across the interface will lead to a charge imbalance. This provides a strong driving force for layer intermixing and the formation of native and extended defects as well as secondary phases [1]. These effects ultimately degrade the interface and the crystalline quality of the overlying semiconductor layer.

The initial growth sequence is known to be crucial for controlling the interface properties as well as the above-mentioned degradation mechanisms. For example, different initiation conditions have been extensively studied in the case of ZnSe/GaAs heterostructures, which is an ideal system due to their nearly equal lattice constants. Zn and Se pre-treatment of the GaAs surface were shown to influence the band-offsets and defect densities in ZnSe epilayers grown on GaAs substrates [2, 3]. However, conflicting conclusions about the effectiveness of these pre-treatments are prevalent in the literature, making it difficult to determine which treatments are most optimal for high quality interface formation [4]. Many of these conclusions were drawn from measurements performed on the ZnSe epilayers. By contrast, very little attention has been paid to the effect of the treatment on the properties of the underlying GaAs. Such information will be valuable for evaluating mechanisms of interface degradation and the effectiveness of each treatment on the interface as a whole, rather than just the ZnSe properties.

Here present an investigation into the growth parameters that affect the formation of ZnSe/GaAs interfaces. Samples were grown on GaAs substrates by molecular beam epitaxy (MBE). The role of As coverage on the GaAs surface and the use of Zn or Se pre-treatment prior to ZnSe layer growth were examined. Low-temperature photoluminescence (LT-PL), X-ray

photoelectron spectroscopy (XPS), atomic force microscopy (AFM), and high-resolution X-ray diffraction (HRXRD) were used to correlate interface stoichiometry with the resulting ZnSe/GaAs interface, as well as ZnSe and GaAs properties. We find that starting with an As-terminated surface is necessary to minimize secondary phase and defect formation at the ZnSe/GaAs interface by moderating Ga-Se bonding. Furthermore, we determine that a Zn pre-treatment is an effective pathway for obtaining high optical and structural qualities of ZnSe which grown on GaAs. Meanwhile, a Se pre-treatment may be more optimal for enhancing excitonic emission from the underlying GaAs.

Experiment

Samples were grown on semi-insulating (100) GaAs substrates in an Omicron EVO25 MBE system with separate III-V and II-VI semiconductor growth chambers. The two chambers were equipped with conventional K-cells for group-III and/or group-II elemental sources and valved cracker effusion cell for the group-V and group-VI elemental sources. The substrate temperature was measured with a k-Space BandiT band-edge thermometry system with an accuracy of ± 1.0°C. The substrates were first outgassed at 300°C in an ultrahigh vacuum chamber before being transferred to the III-V growth chamber, where the oxide layer was thermally desorbed at 610°C for 10 min under an As_2 overpressure. A 500 nm-thick homoepitaxial GaAs buffer layer was then grown, followed by a thick amorphous As layer growth at room temperature for one hour. This layer served to protect GaAs surface as the sample was moved to the II-VI growth chamber, and it also provided a way to vary the GaAs surface from As-rich (Ga-deficient) to As-deficient (Ga-rich). The sample conditions depending on temperature at which As was removed. This “As-desorption” process was carried out at 330 °C, 500 °C or 670 °C in the absence of any group II or VI overpressure. Subsequent growth of the ZnSe epilayer was initiated by one of two pre-treatment methods, as illustrated in Fig. 1. The first method involved a Zn pre-treatment (hereafter referred to as Zn-PT), where the GaAs surface was exposed to Zn for 2 min at 200°C to form a sub-monolayer (ML) of Zn [5, 6]. This was followed by a 30 sec exposure to Se at 200°C, after which the Zn flux was turned back on to grow a thick ZnSe epilayer for 30 min at 300°C. The second method followed a similar procedure, but the Se and Zn exposure order was reversed (hereafter referred to as Se-PT)[7]. The ZnSe epilayer was nominally grown to a

thickness of 130 nm. This value was intentionally chosen to be quite close to its critical layer thickness on GaAs [8] in order to promote a higher sensitivity to changes in the interface and/or surface morphology. Throughout the growth process, reflection high energy electron diffraction (RHEED) was used to monitor the reconstruction of the GaAs surface during the As-desorption, pre-treatment and ZnSe epilayer growth. The layer thickness confirmed by scanning electron microscopy (SEM) image and ω-2θ HRXRD curve simulation. The estimated thicknesses of all ZnSe layers were 2.0 nm (4 ML).

XPS experiments were performed on a Physical Electronics X-ray Photoelectron Spectrometer 5600 equipped with 5-axis sample manipulator, monochromatic AlK_{α} and non-monochromatic MgK_{α} excitation sources. High resolution XPS was obtained with pass energy of 11.75 eV at electron take-off angles of 6º and also 60º relative to the sample surface normal in order to vary the surface sensitivity of the measured signals. A take-off angle of 0º was not available due to the geometry between the monochromatic excitation source and analyzer. Samples were loaded directly from the growth chamber with about 2 minutes of air exposure, and a 5 minute pump down of the load lock prior to introduction to the analyzer, for which measurements were done at $2x10^{-10}$ torr. XPS binding energy calibration was performed on clean Au and Cu metal foils with Au $4f_{7/2}$ at 84.0 eV, and Cu $2p_{3/2}$ at 932.7 eV.

Photoluminescence of the ZnSe epilayers was obtained with a GaN diode laser (405 nm) operated at an excitation power ~1 mW. Two different gratings were used during measurement; 150 l/mm to obtain wide spectral range PL and 600 l/mm to obtain detailed near-band-edge PL of ZnSe. A 435 nm long-pass filter was used to block the laser line. Photoluminescence of the underlying GaAs buffer was obtained with a Nd:YVO laser (532 nm) to avoid pumping the ZnSe epilayer. The excitation power was ~0.31 mW. The measurements were carried out with a 150 l/mm grating and a 570 nm long-pass filter.

Result and discussion

Variation of the surface termination through the As-desorption temperature allows for control over which species are reacted at the GaAs and ZnSe interface. RHEED patterns of the GaAs surface after As-desorption are displayed in Fig. 1 and indicate a change in the As coverage depending on the temperature. A dimeric As covered GaAs surface was obtained immediately

after desorption of the amorphous As layer at the lowest temperature of 330°C based on the RHEED pattern and will hereafter be termed an As-rich surface. As the temperature was increased to 500°C, partial dissociation of dimeric As layer revealed some of the underlying Ga atoms, as indicated by the appearance of a second set of spots in the RHEED pattern. This surface will be referred to as an intermediate surface. At the highest desorption temperature of 670°C, most of the dimeric As was removed, leaving exposed Ga atoms across much of the surface according to the appearance of intense spots in the RHEED pattern that correspond to a Ga atomic surface in RHEED (hereafter referred to as an As-deficient surface).

Figure 2 shows AFM images of the ZnSe surfaces grown after the different interface initiation conditions. Images in the first (a, b, and c) and second (d, e, and f) rows correspond to samples prepared with Zn-PT and Se-PT respectively. The As-desorption temperature increases from 330°C to 670°C from left to right. The small hillocks are SeO_2 islands, which can be formed as soon as ZnSe surface exposed to air [9]. Their contribution to the surface roughness was removed from the following analysis of the surface morphology. All ZnSe samples showed good surface morphology with a small root-mean-square (RMS) roughness comparable to that of a typical homo-epitaxial GaAs buffer layer [10]. Even so, the RMS roughness increased slightly at the highest As-desorption temperatures for both the Zn-PT and Se-PT conditions. This effect was more pronounced in samples fabricated with the Se-PT. We attribute this enhanced roughening to a change in the growth mode from two-dimensional layer-by-layer growth to three-dimensional island growth induced by increased Ga-Se bonding at the interface when the As-deficient surface is exposed directly to Se [11]. This conclusion is corroborated by HRXRD and PL measurements, as discussed below.

Figure 3 shows ω-2θ HRXRD spectra of Zn-PT and Se-PT ZnSe samples. Scans from all samples exhibited a peak -800 arc sec from the GaAs substrate peak, representing a ~0.03% lattice mismatch. However, the HRXRD measurements indicate changes to the interface depending on the initiation conditions. The Pendullösung fringes between the GaAs and ZnSe peaks weaken and the full-width at half-maximum (FWHM) of the ZnSe peak increases with increasing As-desorption temperature under both Zn-PT and Se-PT. These two effects are attributed to the creation of a diffuse ZnSe/GaAs interface and degradation of the ZnSe material quality [12,13], and they are in line with the increase in the RMS roughness observed at high As-desorption temperatures.

Several secondary phases can be formed at the interface between ZnSe and GaAs, depending on which species are permitted to bond. The most prominent include Ga_2Se_3 and Zn_3As_2, with Ga_2Se_3 being the most stable [14, 15]. The elevated density of Ga atoms exposed at the GaAs surface under the highest As-desorption temperature will most readily permit reaction with Se to form Ga_2Se_3. The formation of this secondary phase at the ZnSe/GaAs interface has been linked to the appearance of three-dimensional island growth [11] and deterioration of the ZnSe crystal quality [16], in agreement with our observations. While Se-PT of the As-deficient surface will augment this reaction, Ga_2Se_3 may form to a lesser extent under the other interface initiation conditions. Se is capable of displacing As in the dimeric As layer or As-terminated surface, permitting bonding with Ga [17]. The volatility of Zn_3As_2 created at the interface may also be beneficial for Ga_2Se_3 generation [6]. Formation of this phase through Zn exposure to an As-rich GaAs surface and subsequent evaporation can open up areas of Ga termination that can then react with Se [18]. These alternative pathways to Ga_2Se_3 formation will therefore cause some deterioration of the ZnSe surface morphology and ZnSe/GaAs interface when the interface is initiated with a Zn-PT, although this was observed at a lesser extent than the samples fabricated with a Se-PT. In fact, the spectral width of the HRXRD ZnSe peak expanded more with As-desorption temperature in the Se-PT samples than in the Zn-PT samples, indicating that deterioration of the Se-PT interfaces was much more extensive (Figure 3(b), 3(d)). Thus, suppressing widespread formation of Ga_2Se_3 at the ZnSe/GaAs interface through Zn-PT of an As-rich surface permits two-dimensional growth, ensures high structural quality and yields a smoother surface.

On the other hand, Ga-Se bonding and the formation of Ga_2Se_3 may not always negatively impact the ZnSe/GaAs interface. Comparison of the HRXRD spectra of the Zn-PT and Se-PT samples, the fringes associated with the ZnSe peak extend to greater angle in Se-PT ZnSe samples, suggesting that the interface is more abrupt. To obtain additional information about intermixing at the interface, representative samples were measured by angle-resolved XPS (ARXPS) at high and low electron take off angles. These samples were prepared for ARXPS specifically with ultra-thin ZnSe epilayers to enable the measurement of photoelectrons emitted primarily from the interface. Two 4 ML ZnSe epilayers were grown on Zn-PT and Se-PT GaAs surfaces after As desorption at 300°C. Two take-off angles of 6° and 60° were used to vary surface sensitivity and to determine the interface profile.

XPS spectra were obtained for Ga $2p_{3/2}$, As $2p_{3/2}$, Ga $3d_{5/2}$, As $3d_{5/2}$, Zn $3p_{3/2}$ and Se $3d_{5/2}$ core levels in addition to the C 1s and O 1s core levels. Surface contamination during transfer was found to be less than 2% of the total atomic composition. No secondary phases such as oxides or $GaZnSe_2$ were detected. The spectra are similar to those of ZnSe/GaAs heterostructures presented in the literature [ref], and the kinetic energies and peak binding energies for each of the core levels are reported in Table I. The measurement depths calculated using the TPP-2M equation in the NIST Electron Effective Attenuation Length Database to where 99.0% of the signal is attenuated and are also included in Table 1 and Fig. 4 [C. J. Powell and A. Jablonski, NIST Electron Effective-Attenuation-Length Database, v1.3, SRD 82, National Institute of Standards and Technology, Gaithersburg, MD, 2011]. The Ga $2p_{3/2}$ and As $2p_{3/2}$ photoelectrons were measured from the near-interface region, while the Ga $3d_{5/2}$ and As $3d_{5/2}$ photoelectrons were measured well into the underlying GaAs epilayer. No statistical difference in the $Ga2p_{3/2}/As2p_{3/2}$ and $Ga3d_{5/2}/As3d_{5/2}$ ratios at 6° and 60° take-off angles was detected between the Zn-PT and Se-PT conditions. On the other hand, the Se $3d_{5/2}$ and Zn $3p_{3/2}$ core levels provide a different and deeper observation of the interface when measured at low electron take-off angle. The Se 3d/Zn 3p ratio decreases significantly from 2.66 to 2.19 for the Zn-PT and Se-PT samples respectively for the 6º electron take-off angle. Comparing the more surface sensitive 60º emission angle to the 6º emission angle which probes more of the interface, we assert that the Se enrichment of the interface is significantly increased for the Zn PT. This result suggests that a higher relative concentration of Se has diffused deeper into the GaAs buffer when a Zn-PT is used.

Table I. Binding energies measured by XPS

Element	**Kinetic Energy (eV)**	**Binding Energy (eV)**	**Measurement Depth (nm)**	
			6°	**60°**
Zn ($3p_{3/2}$)	1398	88.6	10.1	5.3
Se ($3d_{5/2}$)	1432	54.1	10.1	5.3
Ga ($2p_{3/2}$)	1468	19.0	3.3	2.2
Ga ($3d_{5/2}$)	370	1117.0	10.0	5.2

As ($2p_{3/2}$)	1446	1322.6	3.3	2.2
As ($3d_{5/2}$)	164	40.7	10.0	5.2

Overall, the XPS results offer clear evidence of intermixing at the interface. The lower Se diffusion into the GaAs when a Se-PT is used is likely result from a higher density of Ga-Se bonds at the interface, which could effectively lock both elements in place and prevent them from diffusing further into the adjacent layers. This then suggest that an As-rich interface and Zn-PT would instead more effectively screen Ga-Se bonding and allow more intermixing to occur, as was also inferred from the HRXRD measurements. Greater intermixing will also lead to a higher chance of forming alloys of various combinations at the ZnSe/GaAs interface that may have residual Zn and/or As. This fact is also discussed in next section.

Because intermixing and defects generated at the interface can strongly influence radiative recombination in both the GaAs and ZnSe epilayers, we explored the effects of the varying interface structure on their emission spectra. ZnSe typically exhibits emission in three distinct spectral regions: near-band-edge emission (NBE), deep level emission (DLE), and Y_0 emission, as shown in Figure 5. The spectra from Zn-PT (Fig. 5a) and Se-PT (Fig. 5c) samples show clear differences in all spectral regions. First, there is a significant difference in the emission intensity and peak energy of the DLE band. They were comparable in the Zn-PT and Se-PT samples prepared with the lowest As-desorption temperature. However, increasing As-desorption temperature in the Se-PT samples leads to a blue-shift in the DLE peak from 2.0 eV to 2.2 eV. Deep level emission in ZnSe has been linked to a variety of impurities and native defects. We have been able to rule out recombination involving Cu due to low levels in our epilayers [19, 20]. Emission in this energy range may also be affected by the presence of Ga impurities. Reference 24 reported that Ga-doped ZnSe exhibited a peak around 2.0 eV when the Ga concentration was high, while a peak around 2.2 eV was more prominent when the Ga concentration was low [21]. In this context, the PL result would indicate that starting with an As-rich GaAs surface before Se-PT permits more Ga to diffuse into the ZnSe layer than an As-deficient surface. This is consistent with the picture that direct Ga-Se bonding at the interface tightly secures Ga atoms in place, preventing diffusion into the ZnSe epilayer and making the interface more abrupt [22, 23].

Y_0 emission is typically correlated with dislocations and other extended defects in ZnSe,

which have been known to be nucleated at Ga_2Se_3 at the ZnSe/GaAs interface [24, 25]. The increase in the Y_0 emission intensity with increasing As-desorption temperature and the use of a Se-PT rather than a Zn-PT can therefore be explained by the higher quantity of Ga_2Se_3 at the ZnSe/GaAs interface under these conditions. Finally, the NBE emission is comprised of donor-bound exciton (DX) and free exciton (FX) peaks, and their intensities also change as a function of As-desorption temperature (Fig. 5b and d). This transformation can be attributed to a competition between emission from shallow states near the band edge and emission from the impurities and native and extended defects that contributes to the DLE and Y_0 bands [21]. Thus, preparation of the ZnSe/GaAs interface with an As-rich surface and a Zn-PT is favorable to realizing ZnSe epilayers with lower impurity and defect densities and higher optical quality. These conditions should be used in cases where the optical properties of the ZnSe epilayer are paramount to device performance.

The optimum growth conditions for improving the optical quality of the underlying GaAs epilayer are different. Figure 6(a)-(c) shows the GaAs near-band-edge emission spectra of the Zn-PT samples prepared under high (670°C), medium (500°C) and low (330°C) temperature As-desorption treatments, respectively. A spectrum of a semi-insulating GaAs wafer used as a reference sample is also shown. Similar to the reference sample, all PL spectra from the heterostructure samples contain peaks associated with bound exciton (BX, 1.515 eV) and carbon bound (C_{As}, 1.490 eV) emission. However, the spectra from the Zn-PT samples contained an additional emission band ranging from 1.40 eV to 1.49 eV. This emission band increased in intensity with increasing As-desorption temperature. Lu et al. reported the presence of a free electron-acceptor emission peak related to Zn-As bonds at ~1.40 eV and the presence of a donor-free-hole emission peak related to Ga-Se bonds at ~1.48 eV [26]. The peak we observe in our samples spans this energy range. Furthermore, its intensity increases with an increase in the As-desorption temperature. We therefore propose that this band is due to recombination in a mixture of Zn-As and Ga-Se bonding environments. The diffuse nature of the interface corroborated by HRXRD and ARXPS measurements suggests there will be a variety of local chemical compositions and bonds over several atomic layers, which could cause emission to occur at energies between these endpoint peaks. More intermixing will then lead to higher emission intensities from these bands, as observed in the sample prepared under the highest As-desorption temperature.

Figures 6(d)-(f) show the corresponding GaAs NBE emission spectra of the Se-PT samples. These samples also exhibited BX and C_{As} emission peaks, but the broad low energy band was absent when the interface was prepared with an As-rich GaAs surface. An increase in the As-desorption temperature to 500°C led to the appearance of a PL peak at 1.48 eV, indicating enhanced recombination at Ga-Se bonds. A further increase in the As-desorption temperature to 670°C then led to the rise of the broad emission band at 1.40 - 1.49 eV. This evolution is expected given that the interface of the samples prepared with an As-deficient GaAs surface and Se-PT will undergo mixing of Ga-Se and Zn-As bonds followed by deterioration of the interface structure altogether. Analysis of the BX emission also indicates that it is preferable to utilize Se-PT to improve near band edge emission in the GaAs epilayer. Comparison of the excitonic emission at 1.515 eV shows that the BX emission is suppressed in the Zn-PT samples while it is enhanced in the Se-PT samples. We therefore conclude from these results that an As-rich GaAs surface and Se-PT are advantageous for suppressing carrier recombination at these low energy states near the GaAs/ZnSe interface.

From our results, it is evident that both the nature of the starting GaAs surface and the pre-treatment are important factors in determining the structure of the interface and the optical properties of the adjacent epilayers. Under all circumstances, maintaining an As-rich surface produced the best results. The effectiveness of the pre-treatment sequence to preserve high optical quality, however, was different for the ZnSe and GaAs portions of the heterostructure. Suppressing Ga-Se reactions at the ZnSe/GaAs interface is advantageous for reducing defects in the ZnSe epilayer and ensuring strong excitonic emission, as determined from HRXRD and PL. We therefore conclude that growing ZnSe after Zn-PT on an As-rich GaAs surface is the best choice in the case where the performance of the ZnSe epilayer matters most for device operation. This is agreement with other II-VI/III-V heterovalent interfaces such as ZnTe/GaSb [27], and Zn pre-exposure help suppressing Ga-Te reaction that can degrade overlying ZnTe epilayer quality [28]. Alternatively, we find that promoting some degree of Ga-Se reaction at the interface is advantageous for creating a more abrupt ZnSe/GaAs interface and reducing impurity diffusion into the adjacent layers due to lattice hardening effects. Thus, a Se-PT may be useful for balancing good excitonic emission with reduced parasitic low-energy recombination in the underlying GaAs. This suggests that an As-rich GaAs surface paired with a Se-PT is advantageous in cases where the optical properties of the GaAs are most important for device

operation (for example: where ZnSe is used only as a cladding layer). Care should be taken when selecting the most optimal interface initiation for the desired application.

Conclusion

In summary, ZnSe epilayers were grown utilizing a variety of interface initiation conditions. They were analyzed by AFM, HRXRD, ARXPS and LT-PL techniques. These measurements revealed that an As-rich GaAs surface is most beneficial for moderating Ga-Se bonding and suppressing the formation of a Ga_2Se_3 secondary phase at the interface that can then nucleate extended defects in the ZnSe epilayer. Further reduction of Ga-Se bonding at the interface by applying a Zn-PT prior to ZnSe growth leads to better structural and optical properties in the ZnSe epilayer. However, promoting some Ga-Se bonding through the use of a Se-PT can improve excitonic emission in the underlying GaAs by reducing the extent of interface intermixing and carrier recombination in a mixed bonding environment. These results can be used to guide the choice of interface initiation conditions for specific applications, where the performance of either the ZnSe or GaAs layers is most important to device operation.

Acknowledgements

We acknowledge the financial support of the Department of Energy Office of Science, Basic Energy Sciences under contract DE-AC36-08GO28308.

References

1. A. Kley, and J. Neugebauer, Phys. Rev. B **50** 8616 (1994).
2. J. Qiu, Q. -D. Qian, R. L. Gunshor, M. Kobayashi, D. R. Menke, D. Li, and N. Otsuka, Appl. Phys. Lett. **56** 1272 (1990).
3. S. Miwa, L. H. Kuo, K. Kimura, T. Yasuda, A. Ohtake, C. G. Jin, and T. Yao, Appl. Phys. Lett. **73** 939 (1998).
4. H. H. Farell, and Randall. A. LaViolette, J. Vac. Sci. Technol. B **22** 2250 (2004) and references therein.
5. M. C. Tamargo, J. L. de Miguel, D. M. Hwang, and H. H. Farrell, J. Vac. Sci. Technol. B **6** 784 (1998).
6. S. H. Islam, M. Tamargo, R. Moug, and J. R. Lombardi, J. Phys. Chem. C **117** 23372 (2013).
7. R. L. Gunshor, L. A. Kolodziejski, M. R. Melloch, and M. Vaziri, Appl. Phys. Lett. **50** 200 (1987).
8. J. Petruzzello, B. L. Greenberg, D. A. Cammack, and R. Dalby, J. Appl. Phys. **63** 2299 (1988).
9. J. B. Smathers, E. Kneedler, B. R. Bennett, and B. T. Jonker, Appl. Phys. Lett. **72** 1238 (1998).
10. B.G. Orr, M.D. Johnson, C. Orme, J. Sudijono, and A.W. Hunt, Solid State Electron. **37** 1057 (1994).
11. Y. Qiu, A. Osinsky, A. A. El-Emawy, E. Littlefield, H. Temkin, and N. Faleev, J. Appl. Phys. **79** 1164 (1996).
12. V. Bousquet, E. Tournié, M. Läugt, P. Vennéquès, and J. P. Faurie, Appl. Phys. Lett. **70** 3564 (1997).
13. L. Tapfer, W. Stolz, and K. Ploog, J. Appl. Phys. **66** 3217 (1989).
14. A. Krost, W. Richter, D. R. T. Zahn, K. Hingerl, and H. Sitter, Appl. Phys. Lett. **57** 1981 (1990).
15. S. Akram, H. Ehsani, and I.B. Bhat, J. Cryst. Growth **124** 628 (1992).
16. A. Coli, E. Carlino, E. Pelucchi, V. Grillo, and A. Franciosi, J. Appl. Phys. **96** 2592 (2004).
17. K. Hellig, G. Prösch, M. Behringer, M. Fehrer, R. Beyer, H. Burghardt, D. Hommel, and D. R. T. Zahn, Appl. Phys. Lett. **71** 2178 (1997).

18. B. Chelluri, T. Y. Chang, A. Ourmazd, A. H. Dayem, J. L. Zyskind and A. Srivastava, Appl. Phys. Lett. **49** 1665 (1986).
19. Y. Shirakawa, and H. Kukimoto, J. Appl. Phys. **51** 2014 (1980).
20. M. Isshiki, T. Yoshida, K. Igaki, Y. Hayashi, and Y. Nakano, J. Phys. C **19** 4375 (1986).
21. B. J. Skromme, S. M. Shibli, J. L. de Miguel, and M. C. Tamargo, J. Appl. Phys. **65** 3999 (1989).
22. T. Yao, M. Ogura, S. Matsuoka, T. Morishita, Jpn. J. Appl. Phys. **22** L144 (1983).
23. N. Kobayashi, Jpn. J. Appl. Phys. **27** L1597 (1988).
24. S. Myhajlenko, J. L. Batstone, H. J. Hutchinson, and J. W. Steeds, J. Phys. C **17** 6477 (1984).
25. B. Buda, O. Leifeld, S. Völlmeke, F. Schmilgus, D.J. As, D. Schikora, and K. Lischka, Acta. Phys. Pol. A, **90** 997 (1996).
26. F. Lu, K. Kimura, S.Q. Wang, Z.Q. Zhu, and T. Yao, J. Cryst. Growth, **184/185** 183 (1998).
27. S. Wang, D. Ding, X. Liu, X. -B Zhang, D. J. Smith, J. K. Furdyna, and Y. -H. Zhang, J. Cryst. Growth **311** 2116 (2009).
28. M. P. Hasall, D. Wolverson, J. J. Davies, B. Lunn and D. E. Ashenford, Appl. Phys. Lett. **60** 2129 (1992).

Figure captions

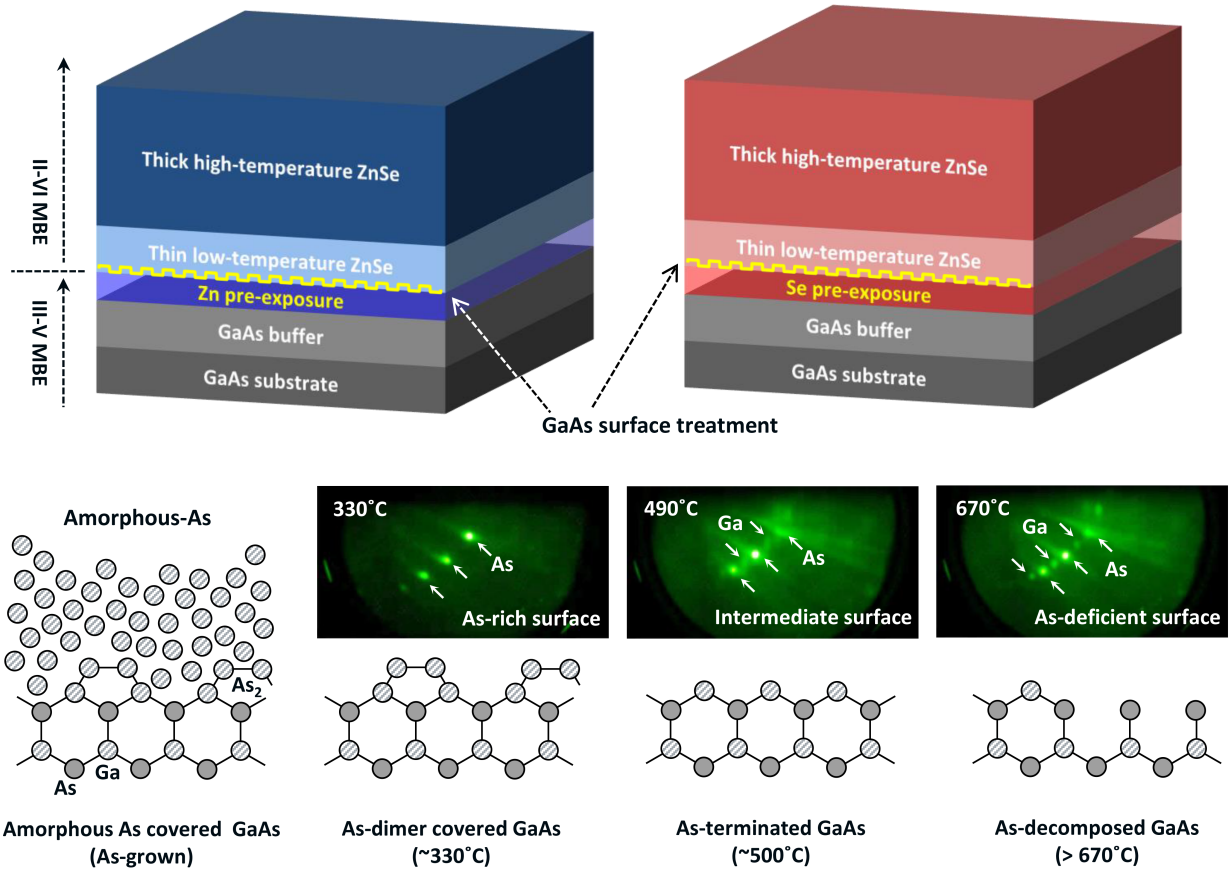

FIGURE 1. (top) Schematics of ZnSe epilayers grown on GaAs substrates with the use of a Zn-PT (left) or Se-PT (right). The As coverage of the starting Gaas surface was also varied from As-rich to As-deficient. These surface coverage conditions were verified by RHEED (bottom).

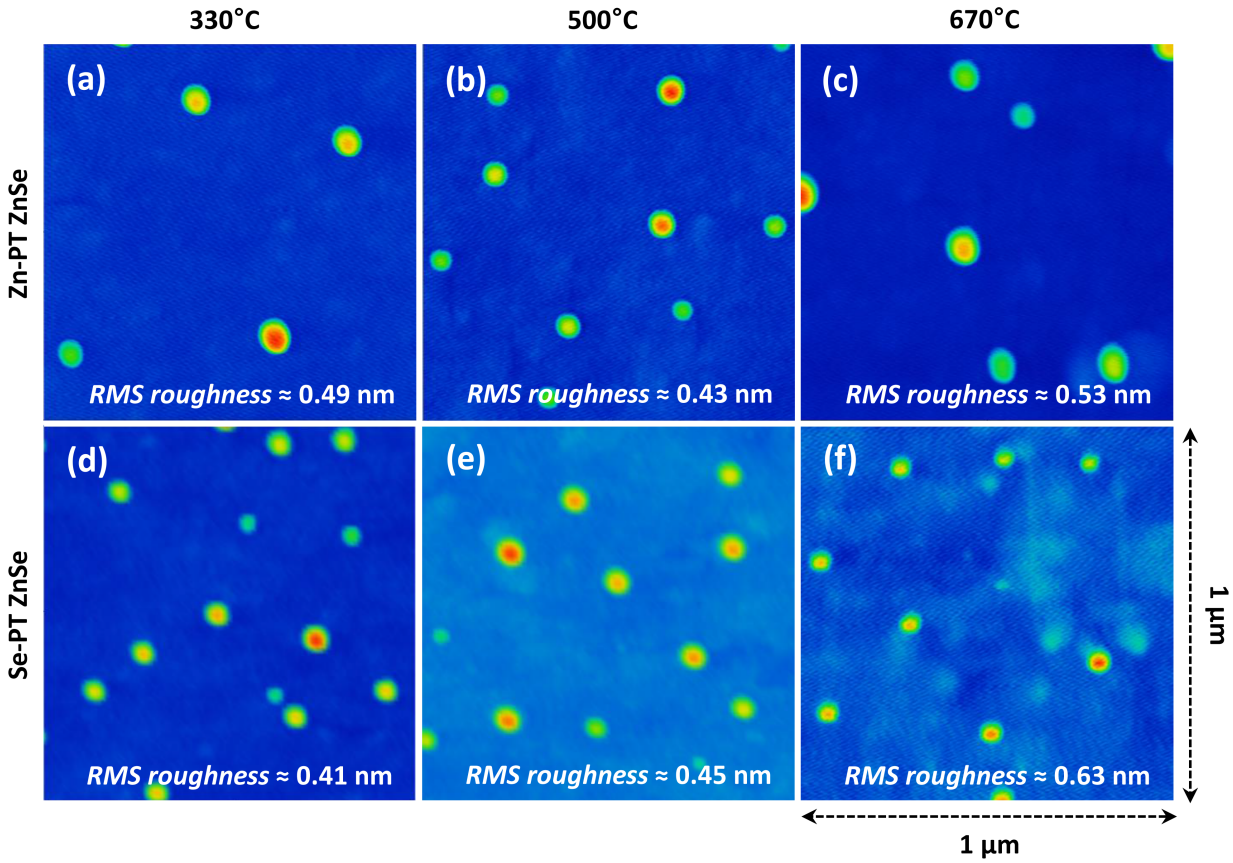

FIGURE 2. 1µm × 1µm AFM images of the ZnSe epilayers grown under various interface initiation conditions. The first row ((a), (b), (c)) and second row ((d), (e), (f)) correspond to samples grown with a Zn-PT and Se-PT, respectively. From left to right, the As-desorption temperature increases from 330°C (As-rich) to 670°C (As-deficient). The RMS roughness is included in each AFM image.

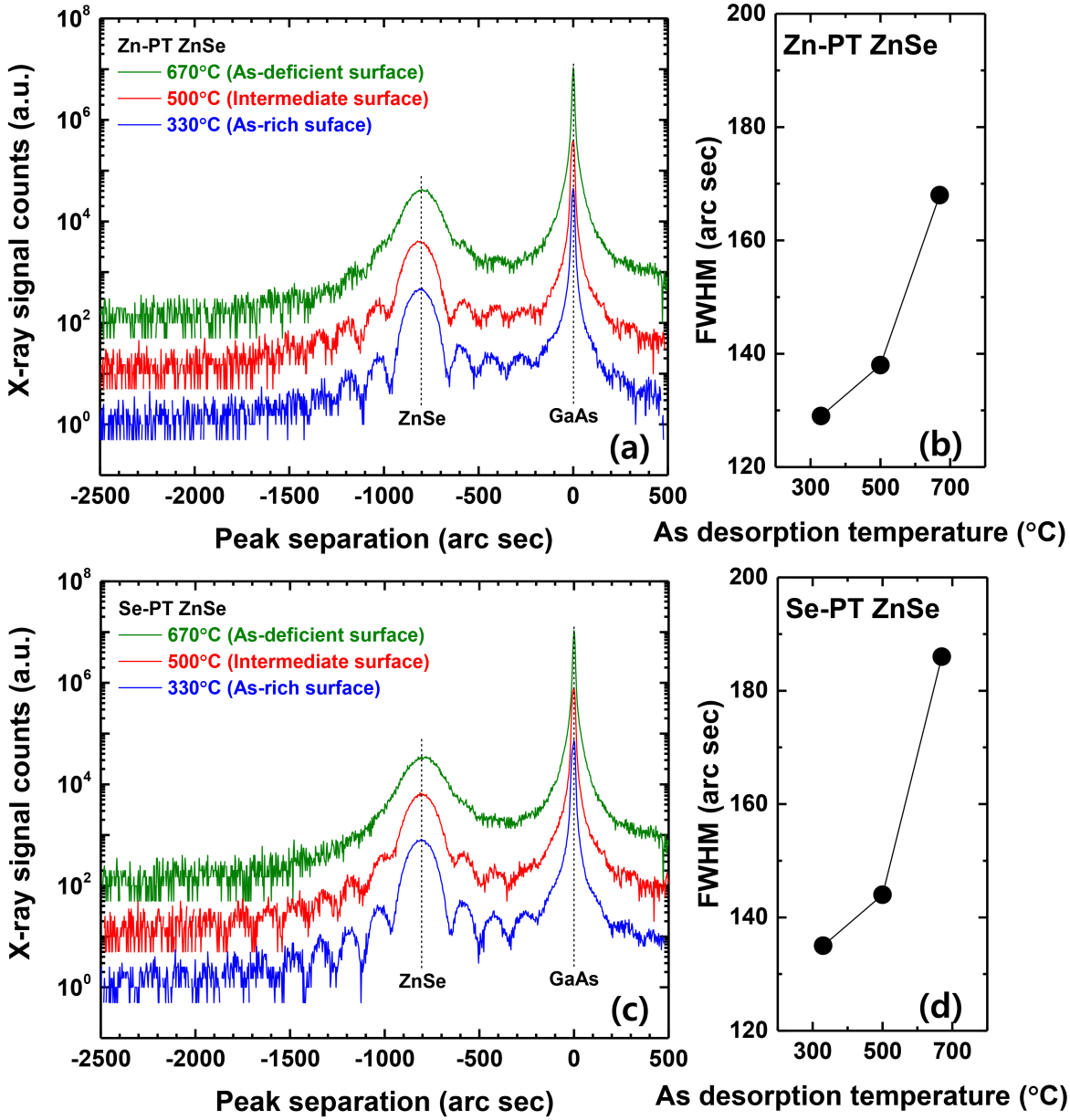

FIGURE 3. (a) and (c) present the HRXRD spectra of samples grown with Zn-PT and Se-PT conditions. The FWHMs of the ZnSe peak as a function of As-desorption temperature for both cases are displayed in panels (b) and (d).

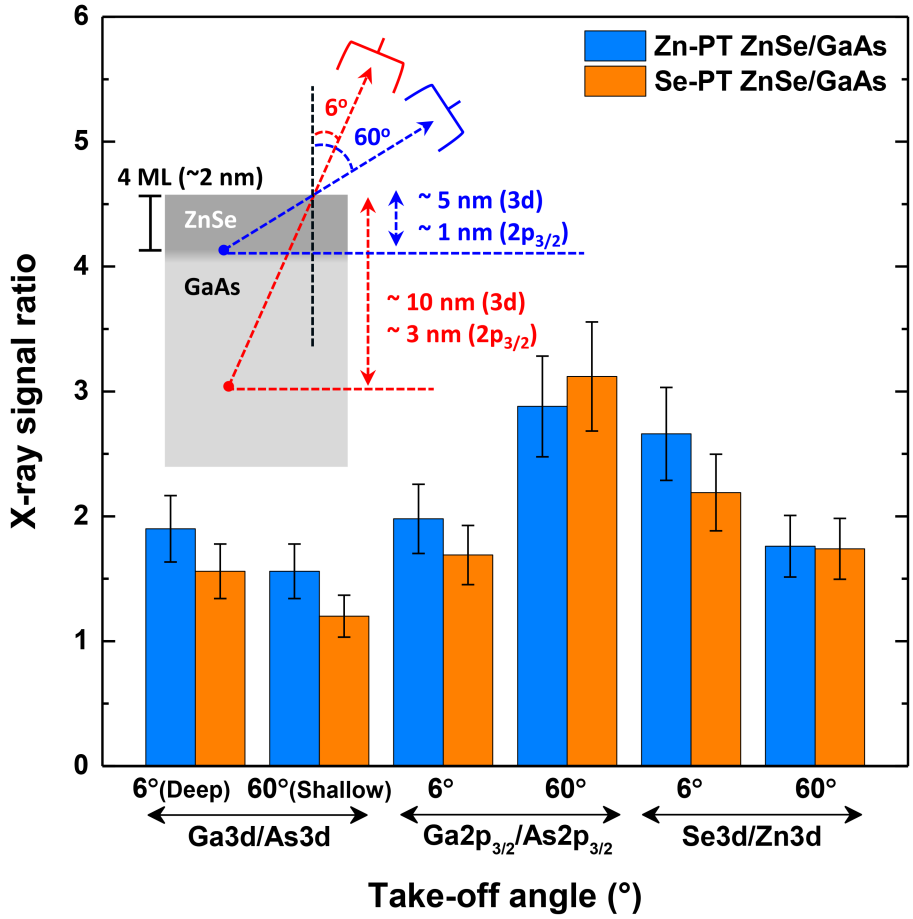

Figure 4. XPS intensity ratios measured as a function of take off angle. (inset) Schematic of measurement and sample geometry, including estimates of measurement depths.

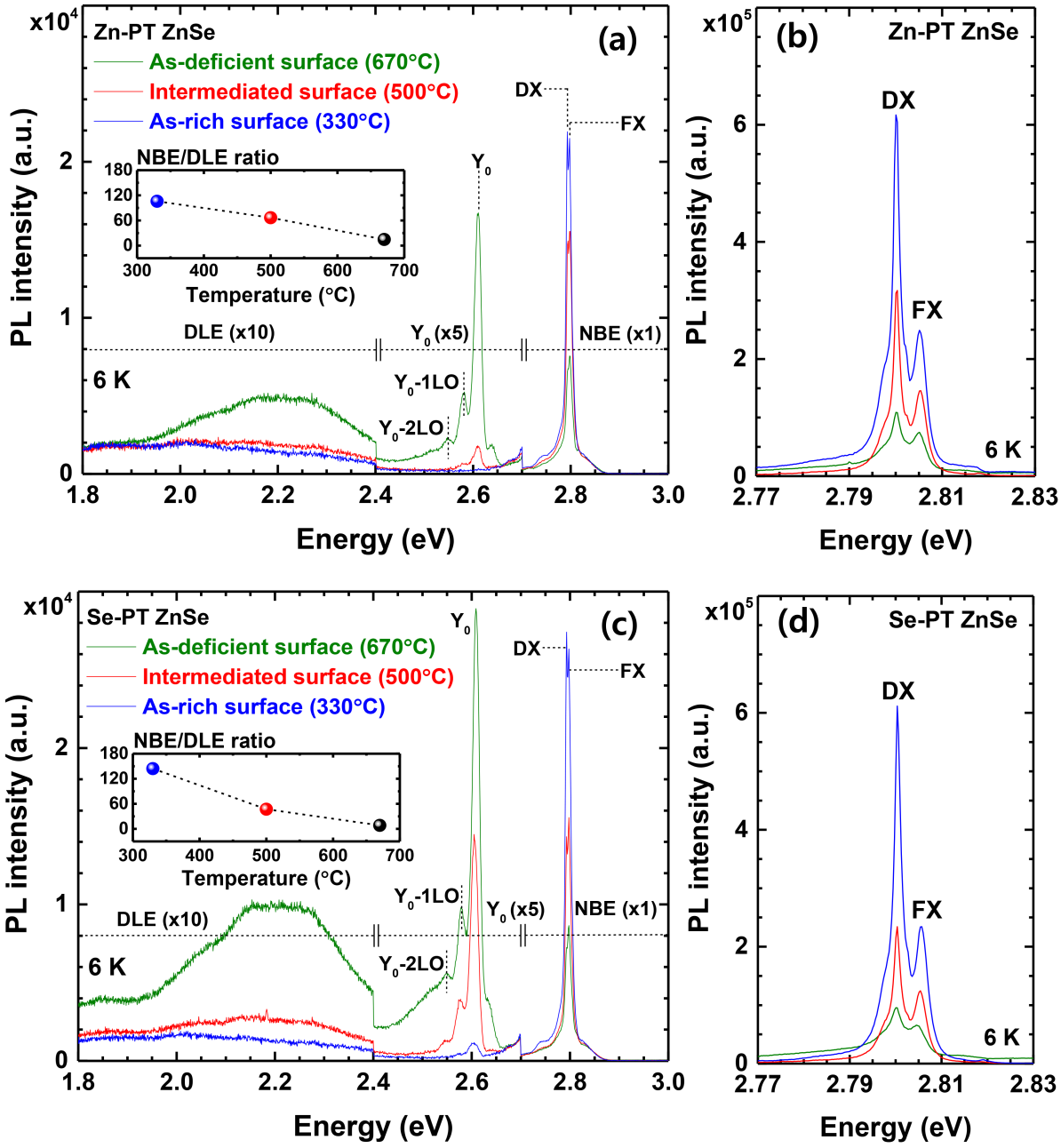

Figure 5. (a) and (c) present the 6 K PL spectra of the ZnSe epilayers grown under Zn-PT and Se-PT conditions. The insets of (a) and (c) display the evolution of the NBE/DLE intensity ratios as functions of As-desorption temperature. (b) and (d) show high resolution spectra of the NBE peaks.

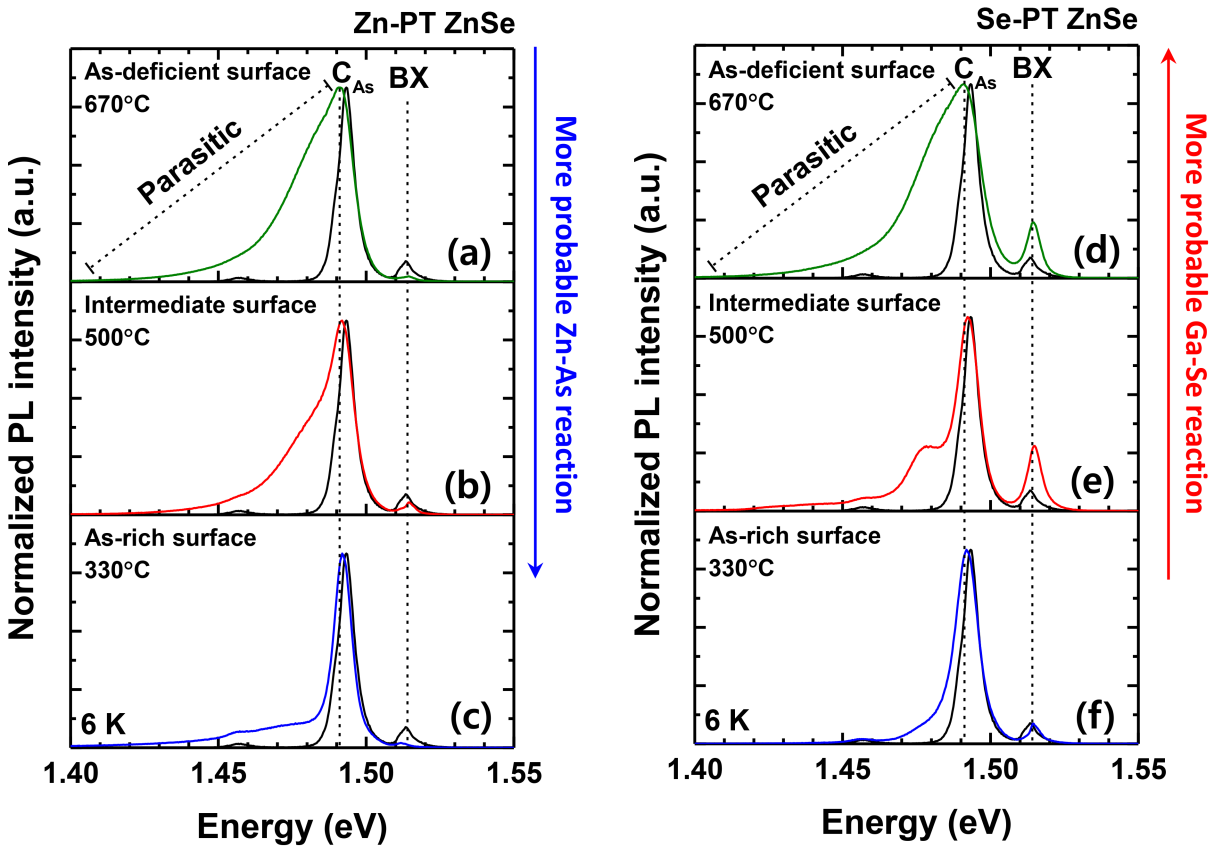

Figure 6. (a)-(c) and (d)-(f) display normalized PL spectra of the underlying GaAs in samples where ZnSe epilayer growth was initiated with a Zn-PT or Se-PT. From bottom to top, the As-desorption temperature increased from 330°C to 670°C.